Proceedings of the European Conference Physics of Magnetism, Poznań 2014

The J_1–J_2 Model on the Anisotropic Triangular and the Square Lattice: Similarities and Differences

B. Schmidt* and P. Thalmeier
Max-Planck-Institut für Chemische Physik fester Stoffe, 01187 Dresden, Germany

The Heisenberg model on a triangular lattice is a prime example for a geometrically frustrated spin system. However most experimentally accessible compounds have spatially anisotropic exchange interactions. As a function of this anisotropy, ground states with different magnetic properties can be realized. On the other hand, the J_1–J_2 model on the square lattice is a well-known example for frustration induced by competing exchange. The classical phase diagrams of the two models are related in a broad range of the control parameter $\phi = \tan^{-1}(J_2/J_1)$. In both cases three different types of ground states are realized, each model having a ferromagnetic and an antiferromagnetic region in the phase diagram, and a third phase with columnar magnetic order for the square lattice and an in general incommensurate spiral structure for the triangular lattice. Quantum effects lift degeneracies in the non-FM phases and lead to additional nonmagnetic regions in the phase diagrams. The contribution of zero point fluctuations to ground state energy, wave vector, and ordered moment is discussed.

DOI: 10.12693/APhysPolA.127.324
PACS: 75.10.Jm, 75.30.Cr, 75.30.Ds

1. Introduction

The two-dimensional anisotropic triangular and J_1–J_2 square-lattice Heisenberg antiferromagnets are two generic models to describe frustration effects in magnetic systems. While the former is the simplest description of a geometrically frustrated spin system with nearest-neighbor coupling, the latter exhibits frustration due to competing exchange interaction between nearest and next-nearest neighbors. Both models have been studied intensively for the case where both exchange constants J_1 and J_2 are antiferromagnetic (AF), where various analytical and numerical methods have been applied. Of particular importance were the isotropic triangular lattice which is believed to have a magnetically ordered ground state with a 120-degree spin structure [1–13], and the square lattice with $J_2/J_1 \approx 0.38 - 0.52$ where a magnetically disordered regime is found [14–17].

In this paper we concentrate on a comparison of the classical and quantum phase diagrams and the size of the ordered moment in the full range of exchange constants, including ferromagnetic (FM) couplings. We apply linear spin-wave (LSW) theory in our analysis, keeping in mind that this method is strictly not applicable in the quantum disordered and (for the triangular case) quasi-one-dimensional regions of the phase diagram. The model Hamiltonian for the lattices is given by

$$\mathcal{H} = \sum_{\langle ij \rangle} \boldsymbol{S}_i J_{ij} \boldsymbol{S}_j, \tag{1}$$

where the sum extends over bonds $\langle ij \rangle$ connecting sites i and j. We assume an interaction in the form of a uniaxial tensor in spin space. Figure 1 illustrates the spatial structure of the exchange, which is

$$J_{ij}^{\square} = \begin{cases} J_1 \text{ if } \boldsymbol{R}_j = \boldsymbol{R}_i \pm \boldsymbol{e}_x \text{ or } \boldsymbol{R}_i \pm \boldsymbol{e}_y \\ J_2 \text{ if } \boldsymbol{R}_j = \boldsymbol{R}_i \pm \boldsymbol{e}_x \pm \boldsymbol{e}_y \end{cases}, \tag{2}$$

$$J_{ij}^{\triangle} = \begin{cases} J_1 \text{ if } \boldsymbol{R}_j = \boldsymbol{R}_i \pm \frac{1}{2}\left(\boldsymbol{e}_x \pm \sqrt{3}\boldsymbol{e}_y\right) \\ J_2 \text{ if } \boldsymbol{R}_j = \boldsymbol{R}_i \pm \boldsymbol{e}_x \end{cases} \tag{3}$$

for the square and triangular lattice, respectively, measuring distances in units of the lattice constants. In order to discuss the full phase diagrams of the models, we use a parameter ζ with $\zeta = 0$ for the triangular lattice, and $\zeta = 1$ for the square lattice. Furthermore we introduce an anisotropy angle ϕ and an overall energy scale J_c defined through

$$J_1 = J_c \cos\phi, \quad J_2 = J_c \sin\phi,$$

$$J_c = \sqrt{J_1^2 + J_2^2}, \quad \phi = \tan^{-1}\left(\frac{J_2}{J_1}\right). \tag{4}$$

This parametrization allows for an interpolation between important geometrical limiting cases, namely the square-lattice Néel antiferromagnet ($\phi = 0$ or $\zeta = 1$, $\phi = \pi/2$), the isotropic triangular antiferromagnet ($\zeta = 0$, $\phi = \pi/4$), the antiferromagnetic chain ($\zeta = 0$, $\phi = \pi/2$), and their ferromagnetic counterparts. The following analysis of the model with the parametrization introduced here closely follows the general concept presented in [18].

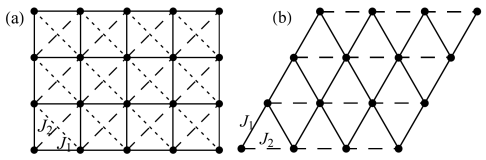

Fig. 1. (a) Square-lattice with nearest-neighbor exchange J_1 (solid lines) and next-nearest neighbor exchange J_2 (dashed and dotted lines). Removing one set of diagonal bonds (dotted) makes the lattice topologically equivalent to an anisotropic triangular lattice (b).

*corresponding author; e-mail: bs@cpfs.mpg.de

TABLE

Classical ground states: energies and conditions. $\zeta = 0$ for the anisotropic triangular lattice ($\triangle$), $\zeta = 1$ for the square lattice ($\square$).

Phase	$E_{\rm cl}/(NS^2)$	Ground state	Conditions	Range
ferromagnet	$2J_1 + (1+\zeta)J_2$	for $\square$ and $\triangle$	$J_1 \le 0 \ \wedge \ \frac{J_2}{\lvert J_1\rvert} \le \frac{1}{2}$	$-\pi - \tan^{-1}\left(\frac{1}{2}\right) \le \phi \le -\frac{\pi}{2}$
antiferromagnet	$-2J_1 + (1+\zeta)J_2$	for $\square$ and $\triangle$	$J_1 \ge 0 \ \wedge \ \frac{J_2}{J_1} \le \frac{1}{2}$	$-\frac{\pi}{2} \le \phi \le \tan^{-1}\left(\frac{1}{2}\right)$
columnar AF	$-(1+\zeta)J_2$	for $\square$ only	$J_2 \ge 0 \ \wedge \ \frac{J_2}{\lvert J_1\rvert} \ge \frac{1}{2}$	$\tan^{-1}\left(\frac{1}{2}\right) \le \phi \le \pi - \tan^{-1}\left(\frac{1}{2}\right)$
spiral	$-J_2\left[1-\zeta+\frac{1}{2}\left(\frac{J_1}{J_2}\right)^2\right]$	for $\triangle$ only	$J_2 \ge 0 \ \wedge \ \frac{J_2}{\lvert J_1\rvert} \ge \frac{1}{2}$	$\tan^{-1}\left(\frac{1}{2}\right) \le \phi \le \pi - \tan^{-1}\left(\frac{1}{2}\right)$

2. Classical phases

The classical energy of Eq. (1) is given by $E_{\rm cl}(\boldsymbol{Q}) = NS^2 J(\boldsymbol{Q})$, where $J(\boldsymbol{q})$ is the Fourier transform of the exchange tensor, Eqs. (2) and (3), and the vector $\boldsymbol{Q}$ can be found by minimizing $E_{\rm cl}$ with respect to it. We find different types of solutions for which the corresponding energies are tabulated in Table, together with the parameter range where the corresponding solution is the actual ground state. Three of these have collinear spin structures, the fourth "spiral" solution denotes a state with an in general incommensurate vector $\boldsymbol{Q} = \boldsymbol{Q}(\phi)$.

Figure 2 shows the ϕ dependence of the classical energies given in Table. The classical phase boundaries of both models are identical, as are the regions where the ferromagnetic or the Néel-type antiferromagnetic solutions are the ground states. For $\tan^{-1}\left(\frac{1}{2}\right) \le \phi \le \pi - \tan^{-1}\left(\frac{1}{2}\right)$, the ground state of the square-lattice model is the columnar antiferromagnet (CAF). This is in contrast to the triangular case, where the spiral phase has minimum classical energy. The difference originates from the "missing" J_2 bonds in the triangular model ($\zeta = 0$ in Table), which raises the energy of the columnar antiferromagnet while lowering the energy of the spiral state.

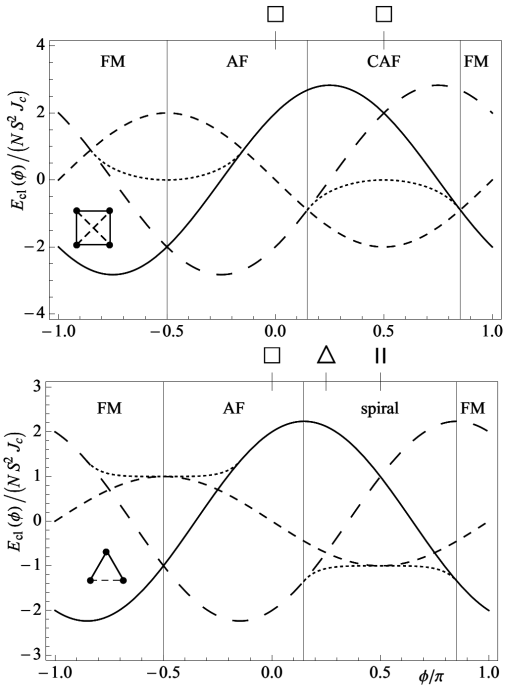

Fig. 2. Dependence of the classical energies given in Table on the parameter ϕ. Solid line: ferromagnet, long-dashed line: antiferromagnet, short-dashed line: columnar antiferromagnet, dotted line: spiral. The vertical lines mark the phase boundaries. Top: square-lattice model, bottom: anisotropic triangular lattice. The symbols above the plots mark the special geometrical limiting cases mentioned in the text.

3. Ordered moment: quantum fluctuations

Quantum fluctuations lead to substantial modifications of the properties of the respective ground states. Of particular interest is the reduction of the size of the ordered moment m_Q from its classical value $m_Q = \mu_{\rm B} S$. We incorporate quantum corrections by applying a Holstein–Primakoff transformation and carry out a large-S expansion, keeping terms up to first order in $1/S$. Details of the procedure are given in Ref. [18].

The size of the ordered moment is eventually given by

$$
\begin{aligned}
m_Q &= \mu_{\rm B} S\left[1 - \frac{1}{2S}\left(\int_{\rm BZ}\frac{{\rm d}^2 q}{V_{\rm BZ}}\frac{A(\boldsymbol{q})}{\omega(\boldsymbol{q})} - 1\right)\right], \\
\omega(\boldsymbol{q}) &= \sqrt{A^2(\boldsymbol{q}) - B^2(\boldsymbol{q})}, \\
A(\boldsymbol{q}) &= J(\boldsymbol{q}) + \frac{1}{2}\left[J(\boldsymbol{q}+\boldsymbol{Q}) + J(\boldsymbol{q}-\boldsymbol{Q})\right] - 2J(\boldsymbol{Q}), \\
B(\boldsymbol{q}) &= J(\boldsymbol{q}) - \frac{1}{2}\left[J(\boldsymbol{q}+\boldsymbol{Q}) + J(\boldsymbol{q}-\boldsymbol{Q})\right], \qquad (5)
\end{aligned}
$$

and the crystal momentum integration is taken over the first Brillouin zone with area $V_{\rm BZ} = 2\sqrt{3}\pi^2$. Figure 3 displays the dependence of m_Q on the model parameter ϕ. Top: square lattice, bottom: triangular lattice. The fluctuation corrections to the classical constant $m_Q/(\mu_{\rm B} S) = 1$ scale with $1/S$, i.e., they are largest for $S = 1/2$ and vanish in the classical limit $S \to \infty$. To illustrate that, we have plotted m_Q for both $S = 1/2$ (solid lines), $S = 1$ (dashed lines), and $S = 3/2$ (bar at $\phi = \pi/4$).

In the FM phase, m_Q remains unmodified because the classical ground state is also an eigenstate of the quantum model. In the AF phase, quantum fluctuations generate a smooth interpolation between $m_Q/(\mu_{\rm B} S) = 1$ and $m_Q/(\mu_{\rm B} S) = 0$. The circles in the plots at $\phi = 0$ denote the well-known value $m_Q/(\mu_{\rm B} S) \approx 0.606$ for the unfrustrated $S = 1/2$ Néel antiferromagnet.

In the CAF phase, apart from the borders, m_Q of the square lattice is almost independent of ϕ, reflecting the small influence of J_1. At the CAF borders,

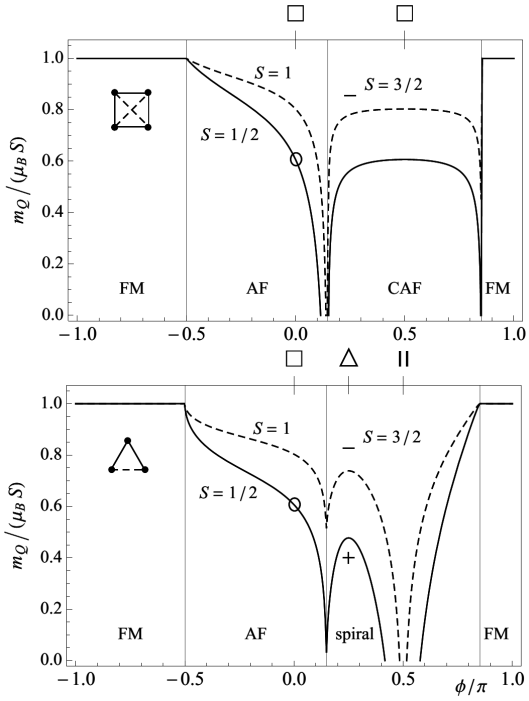

Fig. 3. Size of the ordered moment as a function of the parameter ϕ. Top: J_1–J_2 model on the square lattice. Bottom: anisotropic triangular lattice. The solid lines denote $S = 1/2$, the circle marks the ordered moment for the square-lattice antiferromagnet. The cross marks the DMRG result $m_Q/(\mu_B S) = 0.41$ [5]. The dotted lines show the ϕ dependence of m_Q for $S = 1$, and the bar at $\phi = \pi/4$ denotes m_Q for $S = 3/2$.

the ordered moment vanishes in small areas around $\phi/\pi = \tan^{-1}(\pm 1/2) \approx 0.15$ and 0.85, respectively, giving rise to nonmagnetic columnar-dimer and spin-nematic phases [19].

A completely different behavior is found for the triangular lattice: At the AF/spiral border, m_Q vanishes exactly, and within LSW theory we cannot find an indication for a finite region with $m_Q = 0$. It increases again, passes through a maximum at $\phi = \pi/4$ (isotropic case, 120-degree-spin structure) and is eventually destroyed at $\phi/\pi \approx 0.42$. The maximum value is in reasonable agreement with the DMRG result [5] $m_Q/(\mu_B S) \approx 0.41$ (cross in the plot). At $\phi/\pi \approx 0.58$, m_Q monotonically increases again towards the border of the FM phase at $\phi = \pi - \tan^{-1}(1/2)$. This is opposite to the square lattice, where m_Q breaks down approaching the CAF/FM boundary. The parameter range of vanishing ordered moment corresponding to $J_2/|J_1| \gtrsim 3.9$ denotes a new (classically absent) nonmagnetic phase around $\phi/\pi = 1/2$ with quasi-one-dimensional AF algebraic spin correlations [20]. Because quantum fluctuations decrease, the width of this region becomes narrower with increasing S.

4. Summary and conclusion

We have given an overview over similarities and differences of two important models to describe quantum spin systems: the Heisenberg model on the anisotropic triangular lattice and the frustrated square lattice. We have discussed the classical ground-state energy and the quantum corrections to the ordered moment m_Q due to zero-point fluctuations. Our tool was linear spin-wave theory, allowing for a global investigation with the full range of ferro- and antiferromagnetic exchange couplings. In particular we pointed out the similarity of the FM and AF phases of both models, where the difference originates from the removal of one set of J_1 bonds, having small impact onto ground state and ordered moment. Large differences appear in the region $J_2/|J_1| > 1/2$, where the triangular model shows a strongly nonmonotonic dependence of m_Q on the control parameter ϕ. This includes the breakdown of m_Q around $\phi = \pi/2$ (one-dimensional chains), indicating the appearance of a nonmagnetic phase, where strictly speaking LSW theory is inappropriate and more sophisticated methods have to be applied.

References

[1] T. Jolicoeur, J.C. Le Guillou, *Phys. Rev. B* **40**, 2727 (1989).

[2] A.V. Chubukov, S. Sachdev, T. Senthil, *J. Phys. Condens. Matter* **6**, 8891 (1994).

[3] H. Kawamura, S. Miyashita, *J. Phys. Soc. Jpn.* **53**, 4138 (1984).

[4] B. Bernu, P. Lecheminant, C. Lhuillier, L. Pierre, *Phys. Rev. B* **50**, 10048 (1994).

[5] S.R. White, A.L. Chernyshev, *Phys. Rev. Lett.* **99**, 127004 (2007).

[6] J. Merino, R.H. McKenzie, J.B. Marston, C.H. Chung, *J. Phys. Condens. Matter* **11**, 2965 (1999).

[7] A.E. Trumper, *Phys. Rev. B* **60**, 2987 (1999).

[8] M.Y. Veillette, J.T. Chalker, R. Coldea, *Phys. Rev. B* **71**, 214426 (2005).

[9] M.Y. Veillette, A.J.A. James, F.H.L. Essler, *Phys. Rev. B* **72**, 134429 (2005).

[10] J. Reuther, R. Thomale, *Phys. Rev. B* **83**, 024402 (2011).

[11] Z. Weihong, R.H. McKenzie, R.R.P. Singh, *Phys. Rev. B* **59**, 14367 (1999).

[12] M.Q. Weng, D.N. Sheng, Z.Y. Weng, R.J. Bursill, *Phys. Rev. B* **74**, 012407 (2006).

[13] P. Hauke, *Phys. Rev. B* **87**, 014415 (2013).

[14] G. Misguich, C. Lhuillier, in: *Frustrated Spin Systems*, Ed. H.T. Diep, World Sci., 2004.

[15] S. Sorella, *Phys. Rev. Lett.* **80**, 4558 (1998).

[16] R.R.P. Singh, W. Zheng, C.J. Hamer, J. Oitmaa, *Phys. Rev. B* **60**, 7278 (1999).

[17] H.J. Schulz, T.A.L. Ziman, D. Poilblanc, *J. Phys. I (France)* **6**, 675 (1996).

[18] B. Schmidt, M. Siahatgar, P. Thalmeier, *Phys. Rev. B* **81**, 165101 (2010).

[19] N. Shannon, B. Schmidt, K. Penc, P. Thalmeier, *Eur. Phys. J. B* **38**, 599 (2004).

[20] I. Affleck, *J. Phys. A Math. Gen.* **31**, 4573 (1998).